AGU PUBLICATIONS

JGR

Journal of Geophysical Research: Space Physics

RESEARCH ARTICLE
10.1002/2015JA022080

Key Points:
- Simultaneous observations of the atmospheric electric field
- Downward mapping of ionospheric horizontal electric field
- Magnetic latitude dependence during substorm onset

Correspondence to:
N. J. Victor,
jenivictor@gmail.com

Citation:
Victor, N. J., S. Manu, A. V. Frank-Kamenetsky, C. Panneerselvam, C. P. Anil Kumar, and P. Elango (2016), Network of observations on the atmospheric electrical parameters during geomagnetic storm on 5 April 2010, *J. Geophys. Res. Space Physics*, *121*, doi:10.1002/2015JA022080.

Received 28 OCT 2015
Accepted 4 MAR 2016
Accepted article online 9 MAR 2016

Network of observations on the atmospheric electrical parameters during geomagnetic storm on 5 April 2010

N. Jeni Victor[1], S. Manu[1], A. V. Frank-Kamenetsky[2], C. Panneerselvam[1], C. P. Anil Kumar[1], and P. Elango[1]

[1]Equatorial Geophysical Research Laboratory, Indian Institute of Geomagnetism, Krishnapuram, India, [2]Arctic and Antarctic Research Institute, St. Petersburg, Russia

Abstract The effects of a geomagnetic storm on the variation of the atmospheric electric field over Maitri (70°45′S, 11°44′E), Dome C (75°06′S, 123°20′E), and Vostok (78°27′S, 106°52′E) Antarctic research stations are presented in this paper. For the first time, the paper reports the simultaneous observations of the atmospheric electric field/potential gradient (PG) over the three high-latitude stations at the Southern Hemisphere, and its associated changes due to a substorm phenomenon. PG data obtained from these three stations under fair-weather conditions on 5 April 2010 are analyzed. The duration of geomagnetic disturbance is classified into three intervals, which contains three consecutive substorms based on the magnetic records of the Maitri station. The substorm is directly related to an enhancement of the magnetospheric convective electric field at high latitude, generally controlled by the solar wind parameters. It is found that the variation in the amplitude of PG depends on the magnetic latitude during substorm onset. During the substorm expansion phase, when the convection cell is at overhead, PG is significantly enhanced due to the downward mapping of the ionospheric horizontal electric field. The present observation demonstrated the changes on PG due to the spatial extension of the convection cell from high latitudes up to middle latitudes.

1. Introduction

The fair-weather current, which flows downward from the ionosphere through the atmosphere in fair-weather regions to the Earth's surface, is a good ground-based parameter for probing the ionospheric potential ($V \sim 250$ kV) [*Rycroft et al.*, 2012]. This flow of conduction current in fair-weather regions generates a vertical electric field (E_Z) also known as potential gradient (PG) (potential difference). The PG in fair-weather conditions is typically of magnitude ~120 V/m at 1 m above the surface with the potential increasing positively with increasing height. The main generators which contribute to the global electric circuit are thunderstorms and electrified clouds, which transfer charge from the cloud tops to the ionosphere. Two secondary generators which are more active at middle and high latitudes are the ionospheric tides and the solar wind/magnetospheric dynamo [*Roble and Tzur*, 1986]. The latter generator is active in polar cap regions where the incoming solar plasma perturbs the magnetosphere-ionosphere system via open geomagnetic field lines. This effect is enormously increased during the time of geomagnetic storm and substorm where the tremendous amount of energy is fed into the magnetosphere. The substorm phases (expansion and recovery phases) are generally considered to be the result of a sequence of events that begins with an enhanced coupling of energy into the dayside Earth's magnetosphere [*Bristow et al.*, 2001]. The interaction of the incoming solar wind plasma with Earth's magnetic field causes the existing current systems in the magnetosphere. Due to the high electrical conductivity present along and across the magnetic field lines, any electric fields, generally magnetospheric ($V_{SW} \times B$) origin, produced due to this interaction map to the polar cap ionospheric altitude where they form two cell electric field convection patterns between dawn and dusk. This large-scale (>300 km) ionospheric potential difference maps efficiently downward in the direction of decreasing electrical conductivity toward the lower atmosphere [*Roble*, 1985]. The magnetospheric generator can produce perturbations of ±20% in the current and PG at high latitudes during quiet geomagnetic periods and larger variations during geomagnetically disturbed periods. The development of magnetospheric storms results in the amplification of the ionospheric electric field with an increase in precipitation of energetic particles to the lower ionosphere. This is also suggested to change the conductivity at the lower ionosphere and influences the variation of the electric field at the surface [*Park*, 1976].

Short-term space weather events such as coronal mass ejection (CME) and solar energetic particle events, involving energetic particle precipitation and large-scale ionospheric electric field influence on the current

density and fair-weather electric field measurements, have been shown by *Cobb* [1977] and *Reiter* [1989]. Notably, *Belova et al*. [2001] examined ground level atmospheric current density over Sweden during large magnetic substorm events, finding an increase in atmospheric current density as well as the atmospheric electric field at ground level and suggesting that the enhancement may be due to the downward mapping of the ionospheric horizontal electric field.

Many researchers have investigated the impact of solar wind-induced geomagnetic storms on the atmospheric electrical parameters at middle and high latitudes [*Apsen et al*., 1988; *Nikiforova et al*., 2005; *Kleimenova et al*., 2008; *Smirnov et al*., 2014]. However, there are limited observations on simultaneous measurements of atmospheric electric field, geomagnetic fields, and other geophysical parameters by a network of polar stations over the Arctic regions and USSR. The aforesaid analyses have revealed some common morphological features of electric field disturbances associated with different geophysical conditions. Later digital recording of the field and current in polar regions together has provided many examples of an evident response of the ground electric field to magnetospheric changes induced by solar wind [*Raina*, 1991; *Sheftel et al*., 1994; *Michnowski et al*., 1997]. However, the scope of information from the atmospheric electric field and current measurements on these effects remains limited and analysis of results obtained has not revealed any consistent features. This inconsistency may be due to the complexities of physical processes involved in the near-surface atmosphere for separate geo-effective storms and the selection of the measurement site [*Mikhailova et al*., 2009; *Smirnov et al*., 2013]. Observing the consequences of geomagnetic substorms on the atmospheric electric field or current from the network of stations (latitudinal/longitudinal) is still a difficult task, since the electrical variations are mostly controlled by the local weather conditions. There are few observations that come in the category of discussing the substorm behavior from the Northern Hemisphere [*Odzimek et al*., 2011; *Kubicki et al*., 2014], geomagnetic perturbations from nearly conjugate stations [*Frank-Kamenetsky et al*., 2012]. Particularly, the departure of the atmospheric electric field at middle latitudes due to substorm disturbances was examined by *Kleimenova et al*. [2011] and the similar study had been carried out for large geo-effective storms [*Sheftel et al*., 1992, 1994]. In recent studies, *Kasatkina et al*. [2009] analyzed the solar flare/ground level event's influence on the atmospheric electric field measured from the middle- to high-latitude stations and reported that the changes on the PG are subjected to many factors such as the relative Sun-Earth position, conditions in interplanetary space, and state of the ionosphere and of the atmosphere at middle and high latitudes. Moreover, the magnitude of geomagnetic substorms influencing the atmospheric electrical parameters may vary at different time periods when analyzing multiple stations becomes quite cumbersome. The simultaneous observations of the atmospheric electric field from high latitudes and the effect of magnetospheric/ionospheric generators on the atmospheric electric field are less discussed. Thus, it is reasonable to expect that important and convincing results will come from multistation observations and widely separated atmospheric electric field measurements, which should be able to demonstrate the correlation of surface electric field variations against solar wind variations.

In this study, we report a major geo-effective storm ($Kp = 8$) on 5 April 2010 and its influences on the atmospheric electrical parameters measured at three high-latitude stations on the Antarctic plateau. The observations focus on the latitudinal changes of the ground level electric field for a geomagnetic perturbation, influenced by the solar wind-magnetospheric generator, and its imprint during substorm phases over three widely separated stations in Antarctica.

2. Site Descriptions and Instrumentations

The atmospheric electrical parameters are measured using a variety of experimental techniques, namely, PG, conductivity and air-earth current, which are discussed in many literatures. The Wilson plate [*Israel*, 1973] is the most widely used ground-based sensor for the measurement of air-earth current, and other commonly used sensors are the horizontal long-wire antenna [*Kasemir*, 1955; *Ruhnke*, 1969] and the ball antenna [*Burke and Few,* 1978]. The use of a long-wire antenna in the measurement of air-earth current suppresses the local disturbances as the current is averaged over a large area [*Ruhnke*, 1969].

The Indian Antarctic research station, Maitri, is located in the Schirmacher oasis in the Dronning Maud Land, East Antarctica. Coordinates of the stations are given in Table 1. It is 700 m away from the nearest steep cliff of the east-west trending glacier on the southern side and is 300 m in height. Measurements of surface electric

Table 1. Geographic and Geomagnetic Coordinates of Maitri, Vostok, and Dome C

Station Name	Geographic Coordinates	Geomagnetic Latitude	Height Above Mean Sea Level (m)
Maitri	70°45′S, 11°44′E	67°30′S	117
Vostok	78°27′S, 106°52′E	83°6′S	3488
Dome C	75°06′S, 123°20′E	88°40′S	3250

field have been made by the "Electric Field Monitor (EFM-100) by Boltek," which was installed on a barren land near the station. Description and technical details of the instrument have been reported by *Panneerselvam et al*. [2010]. The surface meteorological parameters like wind speed, wind direction, temperature, humidity, pressure, and all other parameters are systematically measured using an automatic weather station (AWS-PC200).

Vostok is a Russian Antarctic research station located on a high plateau at an altitude of 3488 m above mean sea level. An electric field mill (EFM) was developed by the Science Technical Support group in the Australian Antarctic Division. The EFM instrument measures PG using a spinning dipole technique. The electric field mill consists of a rotating dipole to sense the electric field. This dipole is spun at 1620 rpm. The induced voltage in the dipole is synchronously rectified and digitized. Electric field data are output via a serial interface. The operational height of the EFM is ~3 m from the ice surface, and its sampling interval is ~10 s. Temperature, pressure, and wind speed values are available with 1 min resolution from an automatic weather station (AWS).

Another high-latitude station, Dome C II is a European Antarctic station situated on a flat and icy surface. An electric field mill was deployed at Concordia in January 2008 and functioned until 2013. The EFMs at Vostok and Concordia are of a similar design. Even though the EFMs of the different stations are mounted at various levels, the output data are standardized after applying suitable transfer factors. The standardized data are available for further processing and analyzing.

Antarctica offers a relatively unique location for monitoring fair-weather electric fields associated with the global electric circuit, because it is relatively free from local disturbances such as electrified clouds, man-made atmospheric pollution, etc. The weather is not always favorable for smooth running of experiments due to strong gusty winds (katabatic) reducing the times of the fair-weather measurements. In addition, a higher wind speed (>10 m/s) may alter the electric field measurements when charged blowing snow reaches instrument levels. Moreover, there are occurrences of weather hazards such as fog, snow fall, and blizzard depositing ice/snow on the electric field sensor, so proper care must be taken during these periods to clean and restart the experiments. Periodic cleaning and power maintenance during these days are very much challenging tasks because some of the blizzards continue for more than a week.

3. Data Analysis and Results

Observations of PG over three high-latitude stations are analyzed. The PG data for all the three high-latitude stations are subjected to 5 min averaging. Meteorological parameters were closely monitored to avoid any local effects on the electrical parameters at ground level, so that the variations would be merely attributed to external generators. Solar wind parameters and interplanetary magnetic field (IMF) data are obtained from the NASA OMNI database (http://omniweb.gsfc.nasa.gov/). The 5 min averaged variation of the solar wind and IMF parameters and the geomagnetic indices *Dst*, auroral electrojet (*AE*), *AL*, and *Kp* associated with this geomagnetic storm are shown in Figure 1.

An X-ray flare of the B7.4 class occurred on 3 April 2010, which led to the coronal mass ejection (CME) on 5 April. The incoming solar plasma hit the L1 point at 08:00 UT; it was registered as a sudden increase in solar wind number density (N_{SW}). A sudden shear in the solar wind speed around 08:00 UT is an indication of a traveling shock front, which is marked as dotted line in Figure 1a. It is increased from ~500 km/s to ~700 km/s and reached a maximum of ~800 km/s around 14:00 UT and gradually decelerated. The disturbance further propagated toward the Earth's magnetosphere and produced a sudden commencement on the Earth's magnetic field around 08:27 UT. During an early hour (06:00 UT) of the day, a negative pulse is noticed on the Earth's horizontal magnetic field component measured by a digital fluxgate magnetometer (DFM) at Maitri, which is

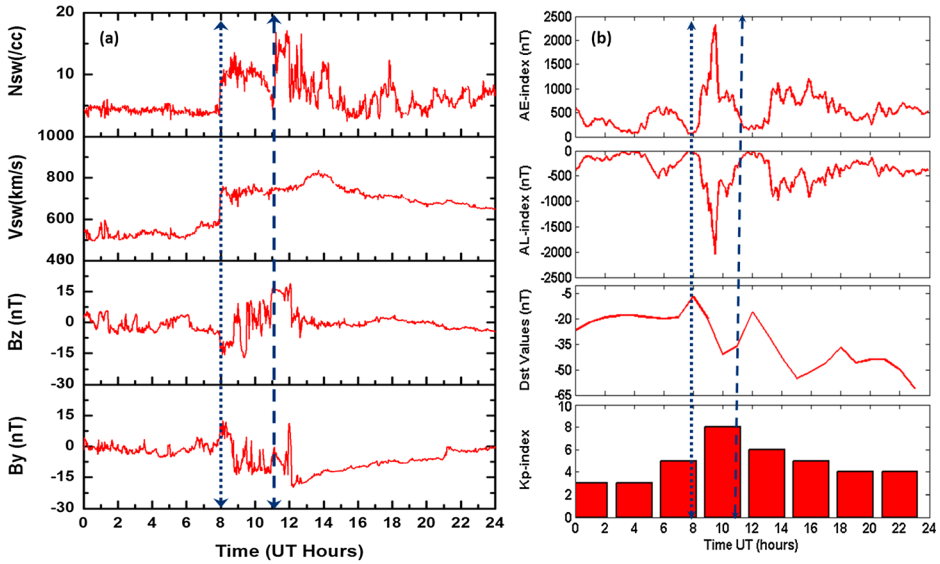

Figure 1. Solar wind parameters, IMF, and geomagnetic index variations on 5 April 2010, where (a) solar plasma number density (N_{SW}), solar wind speed (V_{SW}), interplanetary magnetic field (IMF) north-south component (B_Z) and east-west component (B_Y) and (b) auroral electrojet (*AE*) index, *AL*, *Dst*, and *Kp* indices are depicted from top to bottom.

associated with a small negative impulse in the IMF-B_Z component. This is an initial signature registered on the ground magnetometer on account of the magnetic perturbation.

There are three consecutive substorm negative ΔH bay observed, based on the DFM measurement at Maitri, on 5 April 2010, which is distinguished by three intervals. Interval 1 is from 04:20 to 08:20 UT, where the first substorm corresponds to the time prior to the storm commencement. The second interval is from 08:25 to 11:30 UT where the second substorm corresponds to the time of sudden commencement and its early magnetospheric effects, which were substantially dominated over Vostok, Dome C, and Maitri. The highest level of disturbance has been observed in this interval where IMF-B_Z varied by −15 nT around 09:45 UT along with N_{SW} (~10/cm^3) and solar wind speed (~750 km/s). The change is also observed in *Dst* (−40 nT), *AE* (~2000 nT), and *AL* (−2000) indices as shown in Figure 1b.

The third interval from 11:30 to 13:45 UT corresponds to the magnetosphere response for a solar wind density jump which was observed only over polar cap regions. A strong northward field (IMF-B_Z ~ +15 nT) is observed around 11:30 UT with strong negative IMF-B_Y as indicated by the dashed vertical line in Figure 1a. The fluctuations of B_Z and B_Y components lead to conditions where reconnection occurs near the cusp, generating intense dayside field-aligned currents (FACs) [*Möstl et al.*, 2010]. This magnetic perturbation was recorded on the magnetometer variations from Vostok and Dome C, and the *Kp* index is (~6) also consistent for this variation.

The below section describes in detail the substorm activity with the aid of a ground-based magnetometer and its associated change on PG over three high-latitude stations.

3.1. Maitri

Figure 2 shows the 5 min averaged data of the PG and magnetic field variations measured at Maitri on 5 April 2010. The effects of the geomagnetic substorm on PG may also be sectioned into three intervals. The first interval from 04:20 to 8:20 UT is characterized by a decrease in the horizontal component of Earth's magnetic field. The horizontal component (|Δ*H*|) significantly varied as high as ~150 nT, and its associated changes on PG are meager or absent. However, the occurrence of magnetic perturbation is more distinct from the magnetometer readings as shown in Figure 2 (upper panel).

During the second interval from the time of substorm commencement to 11:30 UT, a small departure of PG followed by a sharp increase in amplitude is observed. It coincides in time with sharp oscillations of the

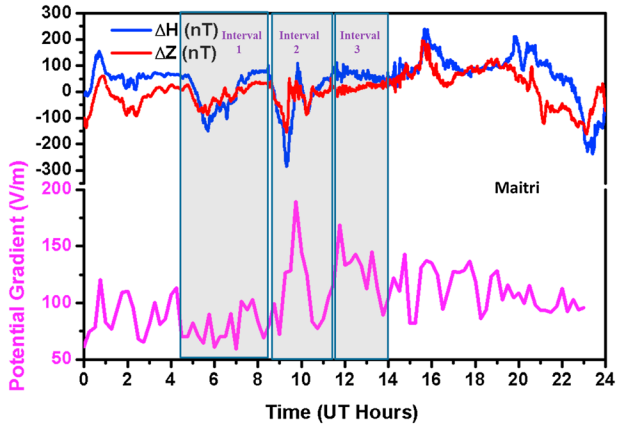

Figure 2. Hourly variation of electric field monitor (EFM) and digital fluxgate magnetometer (DFM) on 5 April 2010 at Maitri.

geomagnetic field (ΔH). Substorm onset was registered in the DFM data at about 08:24 UT, and a simultaneous response was observed on the PG as a small departure around 08:25 UT as shown in the second interval (Figure 2). In the subsequent stages, the influence of the substorm on PG is strong as the intensification of the PG corresponds to the substorm expansion phase. Enhancement on the PG began at about 09:00 UT followed by an intense peak at around ~09:40 UT, where the magnetic disturbances intensified from 09:15 to 09:20 UT as seen in Figure 2. Further, the PG recovered around 11:00 UT followed by a positive enhancement. The later variation on PG may be associated with the change in vertical magnetic field component ($\Delta Z = -76$ nT) around 10: 15 UT.

In the third interval from 11:30 to 13:45 UT, an electric field increase is observed; it may be accompanied by an increase in wind speed/local effect. In order to process the local weather influence on the measured atmospheric electric field at Maitri, the time series of AWS channels are examined. Figure 3 depicts the diurnal variation of wind speed, wind direction, ground level pressure, temperature, and humidity on an hourly scale. In general, fair weather is described as, in the absence of snowfall or fog, cloud cover less than 4 octa and wind speed less than 10 m/s [*Deshpande and Kamra*, 2001].

For the entire period of observations, meteorological parameters were monitored to determine the weather conditions. For example, wind speed varied less than 6 m/s, and later it increased up to 10 m/s from 13:00 UT. The increase in the electric field may be due to blowing snow/space charges as the wind speed increases [*Siingh et al.*, 2013]. Wind speed establishes the strong variations on the PG, and it is noticed at the end of the second interval.

3.2. Vostok

Figure 4 illustrates the diurnal variation of PG and magnetometer at Vostok on 5 April 2010. In the first interval, the PG dropped for the time period of 05:00–06:00 UT where the negative trend of ΔH is observed, which is thought to be an initial sign of substorm activity. However, the variation of the magnetic field to that of the electric field is feeble.

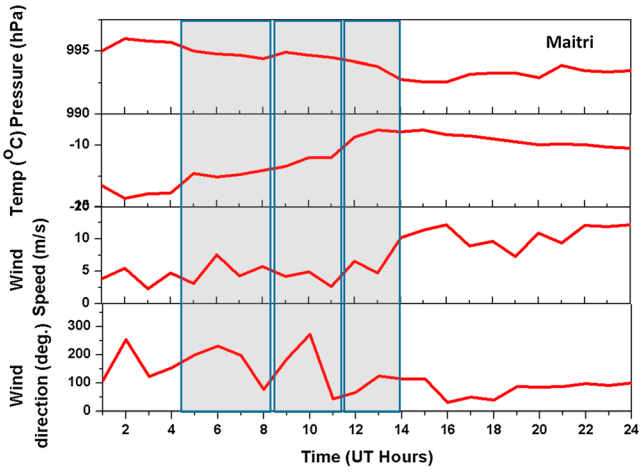

Figure 3. Hourly variation of meteorological parameters from an automatic weather station (AWS) on 5 April 2010 at Maitri.

Substorm onset was noticed around 08:30 UT with a sharp downward trend in the magnetic field components (ΔZ and ΔH), and a simultaneous sharp increase in PG was observed around 08:35 UT over Vostok. Further, it enhanced up to 188 V/m around 08:55 UT, and then the field dropped to 120 V/m at 09:30 UT as depicted in Figure 4 (bottom panel). The horizontal component (ΔH) depicts a long decreasing trend with the maximum amplitude of ~341 nT with an association of IMF-B_Z, where ΔZ negatively peaked (~256 nT) at about 10:00 UT. Vostok PG intensified up to 209 V/m; this increasing phase was

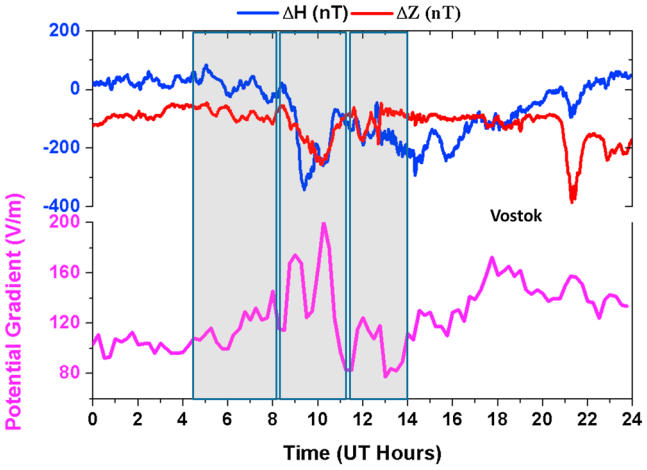

Figure 4. Variation of PG at Vostok and its magnetic field measurement on 5 April 2010.

sustained for more than 30 min in due course. The PG variation during this magnetic disturbances strengthens the earlier observation based on the polar cap potential and IMF parameters over Vostok [*Frank-Kamenetsky et al.*, 2001].

During the next interval, PG decreased around 11:30 UT followed by an enhancement at about 11:35 UT. Double peak variation of PG may be associated with the set of variations observed in solar wind and IMF parameters. The plasma density suddenly enhanced about 3 times higher to that of quiet-time value with IMF fluctuations, marked as a dotted line in Figure 1a. The PG variation over Vostok shown in Figure 4 clearly illustrate the influence of the substorm activity which lasts for two intervals.

AWS data suggest that all the given meteorological parameters satisfy fair-weather conditions over the observing site (Figure 5). Hence, the local effects on PG were minimal on the day of the substorm.

3.3. Dome C

AWS data are not available during the course of time, and the magnetic field measurement also has data gap from the Intermagnet database (http://www.intermagnet.org/data-donnee/dataplot-eng.php) during a few hours of interval. Therefore, the Vostok magnetic field measurement is adopted here as depicted in Figure 6. The DFM data from Dome C and Vostok do not show a signature of the substorm activity during the first interval, unlike at Maitri. Moreover, there are no significant changes observed on the PG at Dome C, and hence, this part of analysis is excluded at this stage. Substorm influence is registered on PG measurement at about 08:32 UT, and after 40 min, it dropped down to ~120 V/m. The maximum departure of PG occurred between 09:40 and 10:20 UT, where it reached up to 266 V/m. The strong perturbation on PG was sustained for almost 2 h, as it varied peak to peak by ~126 V/m. As we have discussed in the last section, the magnetic field variation due to the substorm activity may be the cause for these PG variations and the same may be applicable at Dome C.

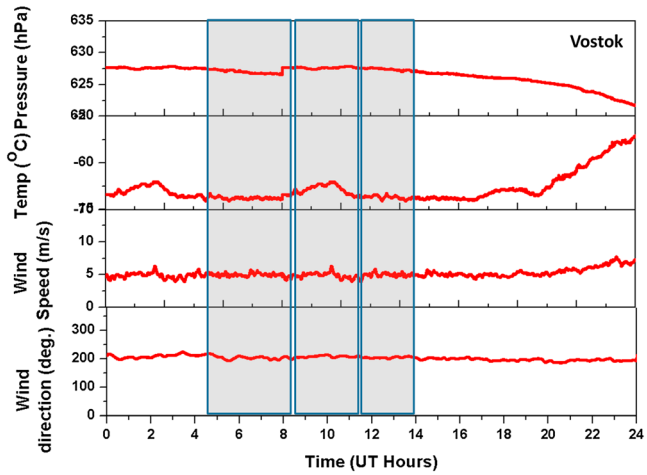

Figure 5. Meteorological parameters measured at Vostok on 5 April 2010.

The final interval of the observation encompassed the increase of PG at about 11:30 UT followed by the two finite peaks observed at 12:00 and 12:30 UT as shown in Figure 6. Subsequently, an enhancement of 110 V/m is observed on PG. During this interval, the electric field varied as high as 171 V/m and as low as 105 V/m with a background field of ~125 V/m.

4. Discussions

We have analyzed the variation of PG measurements from three high-latitude stations during a strong geomagnetic perturbation on 5 April 2010. Investigations of magnetic storms

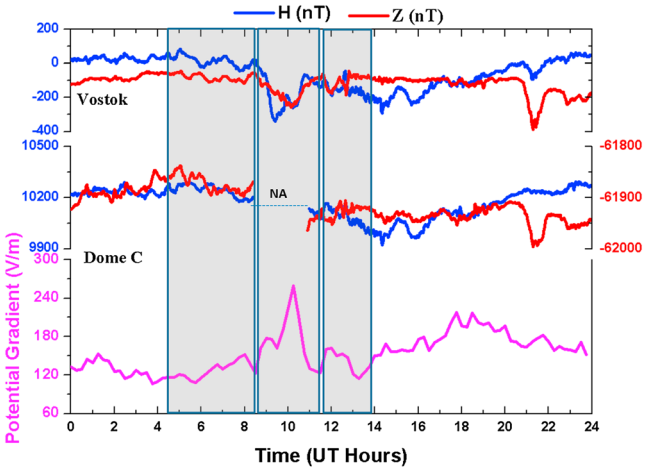

Figure 6. PG and magnetic field measured at Dome C and magnetic field variation at Vostok on 5 April 2010.

on the atmospheric electric field have been discussed in many studies. But the results are inconsistent; it may due to the complexities of the physical process involved in the mechanisms and the choice of the location of measurements. Ultimately, the overall understanding of the physical mechanism is thought to come only if a network of many station observations is possible.

The location of the observatories selected for this analysis are Dome C (magnetic latitude: 88°S; 12 magnetic local time (MLT) = 11 UT) and Vostok (magnetic latitude: 83°S; 12 MLT = 11 UT), situated at the center of the polar cap, and Maitri (magnetic latitude: 67°S; 12 MLT = 11 UT), situated at the equatorward boundary of the auroral zone. Table 1 shows the geographic and geomagnetic coordinates of the three stations. It is inferred from the present analysis that the magnetic field variation and the associated changes observed on PG in each interval are unique for each station. The responding characteristics of PG accompanied with geomagnetic perturbations depend on the magnetic latitude and its local time at the polar cap, auroral, and subauroral zones.

It is understood from the variation in meteorological parameters that local effects are almost negligible during the entire period of observation as shown in Figures 3 and 5. The local dominant factors such as orography, prevailing weather conditions, and elevation of the stations from the sea level may perturb the atmospheric electric field measurement [*Sheftel et al.*, 1994]. In addition to the geomagnetic disturbances on PG, there also exists a day-to-day variability of the thunderstorm electric field [*Tinsley*, 2000].

Figure 7 compares the normalized PG values with respect to its average value (daily mean) from the three high-latitude stations on 5 April 2010. To estimate the deviation of PG from its background field, the so-called thunderstorm-generated electric field, the diurnal average curve of PG at Vostok (April) and the Carnegie curve (average of March-April-May (MAM)) [*Harrison*, 2013] are displayed in Figure 7. During the first interval, the substorm activity is quite unclear, and it seems to be only observed at Maitri, since the other two observatories show insignificant changes in their magnetic field measurements. In addition, the PG observed at the three stations also varied as reference curves (Vostok (April) and Carnegie (MAM)). So the influence of this short-term/small-scale magnetic variation on PG is small compared to other periods and may be indistinguishable from other local effects. It is therefore difficult to determine whether the first interval of the response has any noticeable effect on the PG.

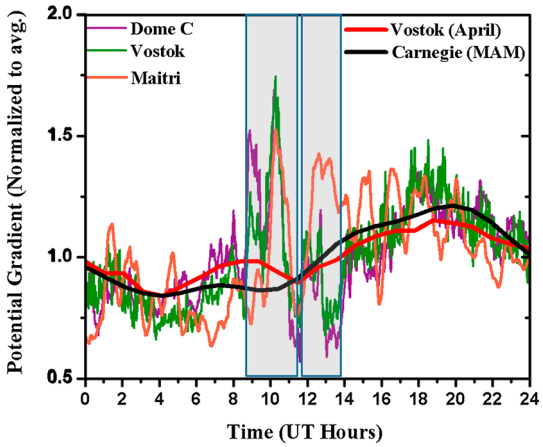

Figure 7. Diurnal variation of normalized potential gradient for three high-latitude stations on 5 April 2010, intervals II and III are shaded. Averaged atmospheric electric field variation on April at Vostok and MAM period from Carnegie observation over plotted.

We have noticed, during the second interval, the substorm signature is recorded on magnetic measurements (DFM) at 08: 25 UT (Maitri), and its associated changes on PG were observed as a peak from 08:30 to 08:40 UT at

Maitri. In general, the onset of a substorm is frequently associated with a southward turn of the IMF-B_Z and it is directly related to the enhancement of the ionospheric convective electric field, which is generally controlled by the solar wind parameters. This ionospheric horizontal electric field is thought to significantly alter the PG measurement at the ground level. It is interesting to note that the PG at Vostok and Dome C is influenced by the substorm onset occurring around ~08:30 UT, where the amplitude varied as high as 185–195 V/m with a background field of 125 V/m (daily mean) as shown in Figure 7. The variation of PG observed at Dome C is rather high compared to that observed at Vostok during the second interval. The departed UT variation of PG with respect to its reference curves is thought to be due to the downward mapping of the solar wind-magnetospheric electric field [*Park*, 1976; *Roble*, 1985]. The southward turning of IMF and enhanced solar plasma density with high speed during this interval are plausible for strong solar wind interaction with the Earth's magnetic field.

Since the magnetospheric convection cell is more active over near-polar-cap regions, a slight change in ionospheric potential difference is sufficient to influence PG measurements at Dome C and Vostok. The difference between the normalized PG and reference curves,

$$\text{Difference} = \text{PGn}((\text{Dome C},\ \text{Vostok},\ \text{and Maitri}))_{\text{UT}} - \text{PGn}(\text{reference curves})_{\text{UT}},$$

at Dome C and Vostok is ~54% and ~28%, respectively.

In the case of Maitri, the variation of PG is fairly less, which is apparent from Figure 7. The subsiding effect of mapping of a large-scale horizontal ionospheric electric field to lower atmosphere may vary from high latitude to subauroral latitude. The effect of coupling of the ionospheric electric field with PG depends on the position of the station with respect to the foci of the convection cells.

In the course of a substorm, the ionospheric electric potential (horizontal electric field) and current patterns over the high latitude consist of two basic components. The first one is related with magnetospheric convection patterns, and the second is the westward electrojet in the dark sector associated with the three-dimensional substorm current circuit. These two components were identified as a signature of the solar wind-magnetosphere-ionosphere interaction [*Kamide et al*., 1994]. The most significant control of instantaneous changes in IMF components on the convection pattern and its associated ionospheric potential difference is expected to occur in the closest region where a direct interaction ($V_{SW} \times B$) is possible (magnetic daytime) [*Frank-Kamenetsky et al*., 1999]. Similarly, during the next course (~09:40–11:30 UT), the gradual changes in the IMF-B_Z maximum of -15 nT significantly enhance the ionospheric potential difference. In addition, a sudden peak signature in the *AE* and *AL* indices around ~09:45 UT suggests that the auroral geomagnetic field responded to the shock front [*Möstl et al*., 2010]. This effect is significantly recorded on ΔH as a strong negative phase, and it depicts the westward motion of the electrojet overhead of measuring site; in other words, the westward electrojet indicates the position of the convection pattern over the station [*Feldstein*, 1991]. In this scenario, it is expected that an intense horizontal electric field exists at the ionospheric altitude, which may produce electrical perturbations through downward mapping. On account of this downward mapping, PG values for Vostok and Dome C are substantially increased 2.2 times than that of the average values (reference curves) at 10:30 UT, whereas Maitri PG increased up to 1.8 times to that of the average. This source of the ionospheric electric field is manifested in the atmospheric electric field (PG) with different weights depending on measurement locations with respect to the magnetospheric convection cell [*Tinsley and Heelis*, 1993; *Michnowski*, 1998]. It is noted that the three observatories were significantly influenced by solar wind-magnetospheric interaction.

The recovery phase of the PG values at 10:45 UT infers that the ionospheric potential is being weakened, and this effect is also consistent with the DFM records by recovery of the ΔH and ΔZ components. A long recovery phase of PG reached well below the ambient values (reference curve). This negative phase, a lesser amplitude than the reference curve at a given UT hour, infers the phase reversal of the superposing downward ionospheric electric field, which may be caused by the polarity changes in the magnetospheric electric field. This strong penetration of the electric field from the interaction of the solar wind and Earth's magnetic field is observed from the polar cap to subauroral latitude. In addition, the weather is also favorable during the course of measurements at all the three stations. Hence, the attenuation ratio for downward mapping due to local weather factors is almost negligible.

In the third interval, PG enhancement is observed at about 11:30 UT at Vostok and Dome C, which is associated with the third magnetic perturbation observed over two stations. A small-scale variation of this magnetic perturbation is inferred from the magnetic field records from Vostok and Dome C as depicted in Figure 6 (top and middle panels). Because the northward (IMF-$B_Z > 0$) and sunward (IMF-$B_Y < 0$) phases of the IMF may confine the plasma motion only over the polar cap regions, this substorm generation is closely associated with the variation of space-time distribution of charged particle precipitations on the upper atmosphere [*Akasofu and Chapman*, 1972; *Kamide*, 1988]. In this context, the IMF-B_Y plays an important role in solar wind-ionosphere coupling, and particularly during large changes of the B_Y component, the ionospheric current and potential distribution patterns undergo drastic changes near the polar cap region owing to polar cap FACs [*Stauning et al*., 1995; *Michnowski*, 1998]. The resultant effect of these current systems was recorded on the magnetometers as two small peaks at 12:00 and 13:00 UT. A similar pattern has also been observed on solar wind density and particularly on the IMF-B_Z parameter as shown in Figure 1a. Interestingly, the PG values obtained from ground measurement have a clear footprint of a similar pattern, which is more apparent from Figures 4 and 6. This observation might strongly pronounce the direct link between PG ground measurement and solar wind-magnetosphere interaction, which has also good agreement with the earlier observations at Vostok [*Frank-Kamenetsky et al*., 1999, 2001].

The magnetic latitudes (~4 latitude degree) of Vostok and Dome C are almost close to the south magnetic pole, where the magnetospheric convection cell is strong and active. Since this third-interval magnetic perturbation seems to occur over polar cap regions, no significant change is observed at the subauroral latitude (Maitri). A particular peak observed on Maitri PG may be attributed to blowing snow/space charges as the wind speed increases.

It is of interest to note that *Smirnov* [2014] reported the variation of the atmospheric electric field measured at Kamchatka (52.9°N, 158.25°E; mag: 46°N) on 5 April 2010. He reported that a sharp PG enhancement was observed during our second interval (08:24–11:30 UT) and no further variations were addressed on account of this geomagnetic perturbation (Figure 2 in the reference), because the magnetic perturbation during the second interval is considerably strong so that its magnetospheric field influence may penetrate up to the middle latitude, which in turn alters the PG. Moreover, the first- and third-interval magnetic perturbations are relatively weak and they have been observed only over high latitudes. Evaluation of these two observations witnesses that the influence of the dawn-dusk potential and its spatial expansion from the magnetic pole (~Dome C-Vostok-Maitri) reached up to 46° (Kamchatka) magnetic latitude. This extension may be even possible at further low latitudes, depending on the level of geomagnetic activity [*Hairston and Heelis*, 1990; *Huang et al*., 2005].

The difficulty in associating auroral and substorm activities with the atmospheric electric field is that the phase and magnitude of the electric field response likely depend on the magnetic local time and location of the site with respect to the auroral substorm [*Kleimenova et al*., 2011].

5. Conclusions

We summarize that the first interval exhibits a substorm activity only at Maitri unlike in Vostok and Dome C. The observed variation on the PG at Maitri is negligible. During the second interval, due to strong substorm activity, significant variations are observed on PG from the three observatories. In the case of the third interval, Vostok and Dome C are under the polar current system and the identified variations on magnetic field and PG measurements are significantly influenced, but Maitri and middle-latitude stations are potentially weak in this regard.

It is inferred that variation in the amplitude of PG depends on the magnetic latitude during substorm onset. During the substorm expansion phase, when the convection cell is at overhead, PG is significantly enhanced due to the downward mapping of the ionospheric horizontal electric field. The deviation of PG with respect to the typical diurnal reference curves clearly indicates that spatial and amplitude variations of the ionospheric convective electric field significantly alter the atmospheric electric field measured over the three high-latitude stations. A network of observatories helps us find the nature of the dawn-dusk convection cell over the observation point. It is still difficult to establish a complete understanding of the observed effects in atmospheric electricity with the help of a single observation. However, these observations are strong enough

to state for the variation of the PG during geomagnetic disturbances. Eventually, for the first time, this analysis demonstrates the influence of the dawn-dusk convection cell from the near-magnetic pole to middle latitude, and it also exhibits the successful downward mapping of the ionospheric horizontal electric field on PG at ground level.

Measurements from three high-latitude stations formed a more reliable data set. It is reasonable to expect that the good amount of significant results emerge from multistation observations and widely separated atmospheric electric field measurements which should be able to demonstrate the correlation of surface electric field variations against solar wind variations.

Acknowledgments

The authors are grateful to Dr. D.S. Ramesh, Director, IIG, for giving permission to publish this work. We greatly acknowledge Prof. S. Gurubaran for his valuable suggestions and guidelines for the improvement of this work. The authors express their gratitude to the Department of Science and Technology (DST), India. The logistic support provided by the Ministry of Earth and Science, Government of India, for conducting a variety of experiments at the Indian Antarctic station, Maitri, is gratefully acknowledged. The authors gratefully acknowledge the valuable remarks of the referees, which helped in making improvements on the original version of this paper. We thank Kyoto WDC (http://wdc.kugi.kyoto-u.ac.jp/) for the *Dst*, *AE*, *AL*, and *Kp* data and the Wind satellite team for the CME and IMF data (http://omniweb.gsfc.nasa.gov/). The electric field mills deployed at Vostok and Concordia were developed under Australian Antarctic Science Advisory Committee Project #974. The Concordia Vertical electric field data collection was approved by IPEV/PNRA Via'Eletricite Atmospherique DC 33 N. Lloyd Symons, Australian Antarctic and Data Division, developed the electric field mill electronics and data collection software. The data for Vostok were obtained from http://data.aad.gov.au/aadc/metadata/metadata_redirect.cfm?md=/AMD/AU/ASAC_974_2 and those for Concordia from http://data.aad.gov.au/aadc/metadata/metadata_redirect.cfm?md=/AMD/AU/ASAC_974_Concordia. The results presented in this paper rely on the data collected at Dome C (DMC). We thank Ecole et Observatoire des Sciences de la Terre for supporting its operation and INTERMAGNET for promoting high standards of magnetic observatory practice (www.intermagnet.org).

References

Akasofu, S.-I., and S. Chapman (1972), *Solar-Terrestrial Physics*, 624 pp., Oxford Univ. Press, New York.

Apsen, A. G., K. D. Kanonidi, S. P. Chernyshova, D. N. Chetaev, and V. M. Sheftel (1988), *Magnetospheric Effects in Atmospheric Electricity*, Nauka, Moscow.

Belova, E., S. Kirkwood, and H. Tammet (2001), The effect of magnetic substorms on near ground atmospheric current, *Ann. Geophys.*, *18*, 1623–1629, doi:10.1007/s00585-001-1623-z.

Bristow, W. A., A. Otto, and D. Lummerzheim (2001), Substorm convection patterns observed by the Super Dual Auroral Radar Network, *J. Geophys. Res.*, *106*(A11), 24,593–24,609, doi:10.1029/2001JA000117.

Burke, H. K., and A. A. Few (1978), Direct measurements of the atmospheric conduction current, *J. Geophys. Res.*, *83*, 3093–3098, doi:10.1029/JC083iC06p03093.

Cobb, W. E. (1977), *Electrical Process in Atmospheres*, edited by H. Dolezalek and R. Reiter, pp. 161–167, Steinkopff, Darmstadt.

Deshpande, C. G., and A. K. Kamra (2001), Diurnal variations of atmospheric electric field and conductivity at Maitri, Antarctica, *J. Geophys. Res.*, *106*, 14,207–14,218, doi:10.1029/2000JD900675.

Feldstein, Y. I. (1991), Substorm current systems and auroral dynamics magnetospheric substorms, *Geophys. Monogr.*, *64*.

Frank-Kamenetsky, A. V., G. B. Burns, O. A. Troshichev, V. O. Papitashvili, E. A. Bering, and W. J. R. French (1999), The geoelectric field at Vostok, Antarctica: Its relation to the interplanetary magnetic field and the cross polar cap potential difference, *J. Atmos. Sol. Terr. Phys.*, *61*(18), 1347–1356, doi:10.1016/S1364-6826(99)00089-9.

Frank-Kamenetsky, A. V., O. A. Troshichev, G. B. Burns, and V. O. Papitashvili (2001), Variations of the atmospheric electric field in the near pole region related to the interplanetary magnetic field, *J. Geophys. Res.*, *106*, 179–190, doi:10.1029/2000JA900058.

Frank-Kamenetsky, A. V., A. Kotikov, L. A. Kruglov, G. B. Burns, N. G. Kleimenova, O. V. Kozyreva, M. Kubitski, and A. Odzimek (2012), Variations in the near-surface atmospheric electric field at high latitudes and ionospheric potential during geomagnetic perturbations, *Geomagn. Aeron.*, *52*(5), 629–638.

Hairston, M. R., and R. A. Heelis (1990), Model of the high latitude ionospheric convection pattern during southward interplanetary magnetic field, using DE2 data, *J. Geophys. Res.*, *95*, 2333–2343, doi:10.1029/JA095iA03p02333.

Harrison, R. G. (2013), The Carnegie curve, *Surv. Geophys.*, *34*, 209–232, doi:10.1007/s10712-012-9210-2.

Huang, C.-S., J. C. Foster, and M. C. Kelley (2005), Long-duration penetration of the interplanetary electric field to the low-latitude ionosphere during the main phase of magnetic storms, *J. Geophys. Res.*, *110*, A11309, doi:10.1029/2005JA011202.

Israel, H. (1973), Atmospheric electricity, Publ Nat Sci Foundation by the Israel Program for *Sci. Transl.*

Kamide, Y. (1988), *Electrodynamic Processes in the Earth's Ionosphere and Magnetosphere, 756*, Kyoto Sangyo Univ. Press, Kyoto.

Kamide, Y., et al. (1994), Ground-based studies of ionospheric convection associated with substorm expansion, *J. Geophys. Res.*, *99*(A10), 19,451–19,466, doi:10.1029/94JA01625.

Kasatkina, E. A., O. I. Shumilov, M. J. Rycroft, F. Marcz, and A. V. Frank-Kamenetsky (2009), Atmospheric electric field anomalies associated with solar flare/coronal mass ejection events and solar energetic charged particle "ground level events", *Atmos. Chem. Phys. Discuss.*, *9*, 21,941–21,958.

Kasemir, H. W. (1955), Measurement of the air-earth current density, in *Proc Conf Atmos. Electricity*, *Geophys. Res. Pap.*, vol. 42, pp. 91–95, Air Force Cambridge Res, Cent, Bedford, Mass.

Kleimenova, N. G., O. V. Kozyreva, S. Michnowski, and M. Kubicki (2008), Effect of magnetic storms in variations in the atmospheric electric field at midlatitudes, *Geomagn. Aeron.*, *48*(5), 650–659.

Kleimenova, N. G., O. V. Kozyreva, M. Kubicki and S. Mihhnowski (2011), Variations in the near-ground electric field at high latitudes and the potential drop across the polar cap during morning polar substorms, *Geomagn. Aeron.*, *51*(3), 397–404.

Kubicki, M., A. Odzimek, N. G. Kleimenova, O. V. Kozyreva, and M. Neska (2014), Synchronization of main global electric circuit generators from ground-level electric field Ez at three distant locations on the globe at middle and high latitudes, XV International Conference on Atmospheric Electricity, 15-20 June 2014, Norman, Okla.

Michnowski, S. (1998), Solar wind influences on atmospheric electricity variables in polar regions, *J. Geophys. Res.*, *103*(D12), 13,939–13,948, doi:10.1029/98JD01312.

Michnowski, S., N. G. Kleimenova, N. N. Nikiforova, and O. V. Kozyreva (1997), The influence of interplanetary magnetic field on atmospheric-electric field in polar regions, Abstracts of the 8th Scientific Assembly Int. Assoc. of Geomagn. and Aeron., Uppsala, Sweden.

Mikhailova, G. A., Y. M. Mikhailov, O. V. Kapustina, G. I. Druzhin, and S. E. Smirnov (2009), Power spectra of thermal tidal and planetary waves in the near-earth atmosphere and in the ionospheric D region at Kamchatka, *Geomagn. Aeron.*, *49*(5), 610–623, doi:10.1134/S0016793209050089.

Möstl, C., M. Temmer, T. Rollett, C. J. Farrugia, Y. Liu, A. M. Veronig, M. Leitner, A. B. Galvin, and H. K. Biernat (2010), STEREO and Wind observations of a fast ICME flank triggering a prolonged geomagnetic storm on 5–7 April 2010, *Geophys. Res. Lett.*, *37*, L24103, doi:10.1029/2010GL045175.

Nikiforova, N. N., N. G. Kleimenova, O. V. Kozyreva, M. Kubitski, and S. Michnowski (2005), Unusual variations in the atmospheric electric field during the main phase of the strong magnetic storm of October 30, 2003, at Swider Polish mid-latitude observatory, *Geomagn. Aeron.*, *45*(1), 140–144.

Odzimek, A., M. Kubicki, M. Lester, and A. Grocott (2011), Relation between the superDARN ionospheric potential and ground electric field at polar station Hornsund, Proceedings of the 14th International Conference on Atmospheric Electricity, 2011, 7-12 August 2011, Rio de Janeiro, Brazil.

Panneerselvam, C., C. P. Anil Kumar, D. Ajay, K. U. Nair, C. Selvaraj, S. Gurubaran, and B. M. Pathan (2010), Instrumentation for the surface measurements of atmospheric electrical parameters at Maitri, Antarctica: First results, *Earth Planets Space*, *62*, 545–549.

Park, C. G. (1976), Downward mapping of high-latitude ionospheric electric fields to the ground, *J. Geophys. Res.*, *81*(1), 168–174, doi:10.1029/JA081i001p00168.

Raina, B. N. (1991), Modulation of global electric circuit by extra-terrestrial influences, *Mater. Pr. Pol. Akad. Nauk Inst. Geofiz.*, *D-35*, 238.

Reiter, R. (1989), Solar activity influences on atmospheric electricity and on some structures in the middle atmosphere, Handbook for Map, 29 J. Laštovička, 168, SCOSTEP, Univ. of Illinois, Urbana.

Roble, R. G. (1985), On solar-terrestrial relationships in atmospheric electricity, *J. Geophys. Res.*, *90*, 6000–6012, doi:10.1029/JD090iD04p06000.

Roble, R. G., and I. Tzur (1986), The global atmosphere electrical circuit, in *The Earth's Electrical Environment*, edited by E. P. Krider and R. Groble, pp. 206–231, Natl. Acad. Press, Washington, D. C.

Ruhnke, L. H. (1969), Area averaging of atmospheric electric currents, *J. Geomagn. Geoelectr.*, *21*, 453–462.

Rycroft, M. J., K. A. Nicoll, K. L. Aplin, and R. G. Harrison (2012), Recent advances in global electric circuit coupling between the space environment and the troposphere, *J. Atmos. Sol. Terr. Phys.*, *90–91*, 198–211.

Sheftel, V. M., O. M. Bandilet, and A. K. Chernyshev (1992), Effects of planetary magnetic storms in the atmospheric electric field near the Earth's surface, *Geomagn. Aeron.*, *32*(1), 186–188.

Sheftel, V. M., O. I. Bandilet, A. N. Yaroshenko, and A. K. Chemyshev (1994), Space time structure and reasons of global, regional, and local variations of atmospheric electricity, *J. Geophys. Res.*, *99*, 10,797–10,806, doi:10.1029/93JD02857.

Siingh, D., R. P. Singh, V. Gopalakrishnan, C. Selvaraj, and C. Panneerselvam (2013), Fair-weather atmospheric electricity study at Maitri (Antarctica), *Earth Planets Space*, *65*, 1541–1553.

Smirnov, S. E. (2014), Reaction of electric and meteorological states of the near-ground atmosphere during a geomagnetic storm on 5 April 2010, *Earth Planets Space*, *66*, 154.

Smirnov, S. E., G. A. Mikhailova, and O. V. Kapustina (2013), Variations in the quasi-static electric field in the near-Earth's atmosphere during geomagnetic storms in November 2004, *Geomagn. Aeron.*, *53*(4), 502–514, doi:10.1134/S0016793213040130.

Smirnov, S. E., G. A. Mikhailova, and O. V. Kapustina (2014), Variations in electric and meteorological parameters in the near-Earth's atmosphere at Kamchatka during the solar events in October 2003, *Geomagn. Aeron.*, *54*(2), 240–247, doi:10.1134/S0016793214020182.

Stauning, P., C. R. Clauer, T. J. Rosenberg, E. Friss-Christensen, and R. Sitar (1995), Observations of solar-wind-driven progression of interplanetary magnetic field B_y-related dayside ionospheric disturbances, *J. Geophys. Res.*, *100*, 7567–7585, doi:10.1029/94JA01825.

Tinsley, B. A. (2000), Influence of solar wind on the global electric circuit, and inferred effects on cloud microphysics, temperature, and dynamics in the troposphere, *Space Sci. Rev.*, *94*(1–2), 231–258.

Tinsley, B. A., and R. A. Heelis (1993), Correlation of atmospheric dynamics with solar activity: Evidence for a connection via the solar wind, atmospheric electricity, and cloud microphysics, *J. Geophys. Res.*, *98*, 10,375–10,384, doi:10.1029/93JD00627.